COMPARATIVE PERFORMANCE OF COMMERCIAL POLYMERIC MEMBRANES IN THE RECOVERY OF INDUSTRIAL HYDROGEN WASTE GAS STREAMS

María Yáñez[1], Alfredo Ortiz[1], Daniel Gorri[1] and Inmaculada Ortiz[1,*]

[1] Chemical and Biomolecular Engineering Department, ETSIIyT, University of Cantabria, Av. los Castros s/n, 39005, Santander, Spain.

Tel.: +34 942 20 15 85; Fax: +34 942 20 15 91; *contact e-mail: ortizi@unican.es

*To whom correspondence should be addressed.

International Journal of Hydrogen Energy

ABSTRACT

The application of membrane separation processes to industrial hydrogen-rich waste gases promotes the efficient recovery of this clean fuel. The first step to address and overcome this waste of resources is to assess the real performance of commercially available polymeric membranes for hydrogen separation in terms of hydrogen purity that meets the quality standards to be used in hydrogen-based applications. Therefore, this work makes a comparison of the performance of commercial flat hydrogen-selective membranes based on non-porous polymeric materials through the experimental assessment in a lab-scale set up that contains a gas permeation cell with the aim of recovering hydrogen from the most suitable multicomponent waste gaseous streams. To assess the mixed-gas permeation performance, the influence of the feed gas composition, temperature and pressure was examined. The results of experimental tests indicated that there is a strong dependency of H_2 permeability on CO_2 concentration, that induces a decay of H_2/CO_2 selectivity in mixed-gas experiments for the membranes under study. Accordingly, the permeability-selectivity trade-off in the state-of-the-art membranes defines the balance between H_2 recovery and the product purity. Finally, it is worth noting that although H_2 purities obtained are higher than 98 % vol. H_2 for APG and COG mixtures, which may indeed be used as a commodity chemical in many industrial processes, they are still far from fuel cell requirements.

KEYWORDS

Hydrogen separation, industrial surplus hydrogen, polymeric membranes, mixed-gas permeation.

1. INTRODUCTION

Interest in hydrogen has been growing over the past decade as a way of enabling a full large-scale integration of renewables in response to decarbonize the energy system and concerns about the depletion of the world's fossil fuels reserves [1]. While much of the hydrogen is currently produced from low-cost natural gas, hydrogen production from carbon-lean and carbon-free energy sources has the potential to serve as a long-term environmentally friendly alternative in a truly sustainable energy system [2]. Despite a large industrial market dominated by refineries and chemical plants, niche markets for hydrogen are likely to emerge in the short-to-medium term.

At the same time, up to 0.5 Mt H_2 produced worldwide is currently vented to the atmosphere from several industrial users, while 22 Mt H_2 is simply used for on-site heat and power generation, even though cheaper energy sources could be used instead [3]. With the aim of tackling this waste of resources, this available surplus hydrogen, that in some cases is simply vented or flared to the atmosphere, has also become an attractive source of feedstock for the manufacture of commodity chemicals in many industrial processes, or even to be upgraded to fuel for both transportation and stationary applications [4]. A previous study from our group showed that the use of inexpensive surplus hydrogen sources offers an economic approach to cover hydrogen demand in the very early stage of transition to the future global hydrogen-based economy [5].

At the point of use, within the numerous hydrogen-based applications, hydrogen fuel index should comply with ISO 14687 standards, which states a hydrogen fuel index of 98% to feed conventional internal combustion engines (ICE) (Type I, Grade A), of 99.9 % for proton exchange membrane fuel cell (PEMFC) stationary appliance systems (Type I, Grade E), and of 99.97 % for PEMFC road vehicle systems (Type I, Grade D) [6–8]. Depending on the industrial origin, low-quality hydrogen streams, which could contain different types of contaminants, need to be purified using gas clean-up technologies [9].

A broad range of technologies, i.e. pressure swing adsorption (PSA), membrane systems and cryogenic distillation, are available in the market and compete each other for hydrogen upgrading purposes. The advantages of membrane technology over existing separation processes, such as high selectivity, low energy consumption, small footprint, moderate cost to performance ratio and compact and modular design, especially in small to medium capacity plants, have been widely reported [10]. A number of comprehensive reviews have been conducted on membrane sciences for hydrogen purification during the last few years [11–15]. These studies have identified three kind of

membranes based on the materials, which are of polymeric, inorganic and metallic nature. These membranes differ in terms of the hydrogen separation performance and the applicable operating conditions [16]. Compared with metal and inorganic membranes, dense, organic (polymeric) membranes (DPMs) are the dominating materials for gas separation membranes at present, due to their lower material and manufacturing costs and competitive performance (mild operating conditions) [17]. Although metal membranes, such as palladium-based membranes, could provide infinite permselectivity of hydrogen, apart from its inherent material cost, they are more suitable for use at high operating conditions (> 300 °C) to avoid embrittlement [18]. After many years of development, membrane separation technology has been extensively applied in many industries with moderate hydrogen purity requirements, especially for natural gas upgrading/sweeting (90 % purity), and also as fuel gas (54 – 60 % purity). As a matter of fact, membrane manufacturing companies use a quite limited set of polymers as hydrogen-selective membrane materials such as polysulfones (PSF), polycarbonates (PC), cellulose acetates (CA), polyphenyloxides (PPO) and polyimides (PI), meanwhile new high performance tailor-made polymers are still under intensive research and development, but currently most of them are too expensive to be used at large scale [19].

However, membrane processes have several inherent limitations such as the moderate purity reported by state-of-art hydrogen-selective DPMs working with low pressure permeate at mild temperature conditions. This is because among the vast amount of polymers that have been investigated, the general trend shown is that highly permeable polymers possess low selectivities. Moreover, the permeability and selectivity of a membrane vary under different operating conditions (temperature, pressure, humidity and gas compositions, etc.) [17]. Thus, further research on the assessment of the performance of the available hydrogen separation membranes under different conditions is also a crucial factor for determining the feasibility of the membrane process for a specific industrial application. Furthermore, as for gas mixtures, the transport behavior of one component through the membrane is affected by the presence of other penetrants, which resulted in deviations from permeation data of pure gases. In addition, the non-ideal gas behavior of CO_2-containing mixture and the concentration polarization phenomenon, also cause the deviation from permeation data of pure gases [20]. Hence, using single gas permeation data to estimate the performance of gas mixtures may lead to confusing results and, for that reason, the membranes behavior during mixed gas measurements must be thoroughly analyzed [21,22].

Hence, in the present work, we aimed to test conventional DPMs using synthetic multi-component gaseous mixtures based on three of most suitable industrial hydrogen-rich waste gases, which compositions and outlet conditions are detailed in Table 1. No study in the open literature, to our knowledge, has investigated the mixed-gas permeation behavior on polymeric membranes for these specific gas mixtures, which have been identify as the industrial waste gases with major potential for hydrogen upgrading processes. The first source of hydrogen off-gas corresponds to a hydrogen-containing gas stream purged at high pressure during the ammonia synthesis to keep the inert gases concentration below a threshold value [23,24]. These ammonia synthesis vent gases are often called as ammonia purge gas (APG). In more recent designs, this hydrogen is mostly recovered and recycled to the synthesis loop via membrane contactors or cryogenic systems, but some part of the cleaned purge gas is usually added to the reformer, or even directly released to the atmosphere [25,26]. Another hydrogen-rich gas stream is a purge stream, called methanol purge gas (MPG) stream, produced during methanol synthesis, which is purged to maintain the syngas rate within the methanol production unit [27,28]. Even though, MPG is often valorized within several internal process steps; but also, some part is burnt in the flare. Finally, coke oven gas (COG) is a by-product of coal carbonization to coke, which is co-generated in the coking process. Nowadays, this gas is simply used as fuel for the under-firing of coke oven batteries, in which only the calorific value of this stream is used for power generation, as well as in other processes of the steel plants, but still only accounts for approximately 20 – 40 % of the total COG produced in coking plants [29,30]. Thus, very often the excess of COG cannot be used in this way and so it is burnt directly in flare stacks, followed by discharged into the atmosphere [31]. In all cases, output flow conditions are generally at ambient temperature, which makes DPMs suitable for hydrogen recovery.

Table 1. Case study industrial waste gas streams parameters

		Gas composition (% vol.)						
Industrial sources	**ID**	**H_2**	**N_2**	**CO_2**	**CO**	**CH_4**	**T (°C)**	**P (bar)**
Ammonia industry	APG	58.6	25.7	-	-	15.7	15 - 30	> 100
Steelmaking process	COG	60.2	4.7	2.1	6.8	26.2	15 - 30	5 - 20
Methanol production	MPG	63.1	11.3	11.1	3.4	11.2	15 - 45	70

In this way, a comparative performance analysis of commercially available polymeric membranes for hydrogen separation is developed, and applied to industrial waste gas mixtures to obtain high-purity hydrogen. Therefore, the aim here is to investigate the permeation of pure gases and multicomponent mixtures of H_2, N_2, CH_4, CO, and CO_2 at different operating conditions through dense polymeric films. Furthermore, the impacts

of other important process parameters such as temperature and pressure on the performance of the membranes are investigated. Hence, new knowledge on membrane behavior related to real process conditions are revealed for commercially available DPMs. The results render to the status of a membrane-based hydrogen recovery process applicable to industrial-scale waste gas streams.

2. EXPERIMENTAL PROCEDURE

2.1. Theoretical background

Gas transport in DPMs is mostly described by the solution-diffusion mechanism. In this case, the permeating gas dissolves into the polymer at one face of the membrane, diffuses across the membrane and then is desorbed at the downstream face. Thus, permeability is a function of both gas diffusivity and solubility [32]. Whereas the order of gas permeability in rubbery polymers (polymers with glass transition temperatures, T_g, below the operating temperature) is governed principally by gas condensability, in glassy polymers (polymers with T_g above the operating temperature) the order is related to the size difference between the gas molecules and the size sieving ability of the polymer [12]. Glassy polymers that are generally used for fabricating H_2-selective membranes exhibit higher thermal stability compared to rubbery polymers, which are used for CO_2-selective membranes [33]. Moreover, H_2-selective membranes are able to tolerate higher compression stresses from high-pressure feed streams [34, 35].

Concerning the theory, less condensable gases (i.e. H_2, N_2) with very low solubility in polymeric materials, they only weakly affect the property and behavior of polymers, and do not influence the mutual diffusion and solubility parameters in the process of simultaneous transport of gases in mixture separation. For more condensable gases (i.e. CO_2) with great solubility, the applicability of ideal permeation parameters is less predictable [33]. The following formula is used to calculate the gas permeability coefficients for multicomponent gas mixtures [36,37]:

$$P_\mathrm{i} = \frac{{Q_\mathrm{i}}^P \cdot \delta}{A \cdot \Delta p_\mathrm{i}} = \frac{{Q_T}^P \cdot {x_\mathrm{i}}^P \cdot \delta}{A \cdot (p^F \cdot {x_\mathrm{i}}^F - p^P \cdot {x_\mathrm{i}}^P)} \qquad \text{Eq. (1)}$$

where P_i is the mixed-gas permeability coefficient of component i, a normalized measure of permeation flux through the membrane. It is expressed in Barrer (10^{-10} cm^3 (STP) cm cm^{-2} s^{-1} $cmHg^{-1}$). The permeability is related to the permeation flux of a gas component i referred to standard conditions through the membrane ${Q_\mathrm{i}}^P$ (cm^3 (STP) s^{-1}),

the area of the membrane A (cm^2), the selective layer thickness of the membrane δ (cm), and the driving force for separation Δp_i (cmHg), is the gas component i partial pressure gradient across the membrane. Likewise, ${x_i}^F$ and ${x_i}^P$ are the mole fraction of component i in the feed and permeate stream, respectively. The mixed gas selectivity is defined as the ratio of permeability values and it can be expressed in terms of measurable variables in the experiments, as follows:

$$\propto_{i/j} = \frac{P_i}{P_j} = \frac{{x_i}^P \cdot (p^F \cdot {x_j}^F - p^P \cdot {x_j}^P)}{{x_j}^P \cdot (p^F \cdot {x_i}^F - p^P \cdot {x_i}^P)} \quad \text{Eq. (2)}$$

where ${x_j}^F$ and ${x_j}^P$ are the mole fractions of component j in the feed and permeate stream, respectively.

2.2. Dense polymeric membrane materials

The first step consist of making a comparative analysis of available polymeric membranes in order to select the material that offers the best performance for hydrogen recovery from aforementioned waste gas streams. Due to the relative high hydrogen content within the gas mixtures exhausted under mild temperature conditions, and also the required high-purity hydrogen to comply with ISO 14687 series, a polymer with high selectivity towards hydrogen and reasonable permeability over a long period of usage is needed. Also, materials should be processed into thin, typically supported membranes, fashioned into high surface/volume ratio modules (up to 30.000 $m^2\ m^{-3}$ of packing density for hollow fiber (HF) modules), and used in optimized processes [38].

At this point, gas permeation properties of various commercial polymers have been compiled by plotting the selectivity of different gas pairs versus the H_2 permeability in Robeson-type plots, as depicted in Figure 1. All gas permeability data were taken from Membrane Society of Australasia (MSA) database [39]. Although very limited research works have addressed the mixed permeation of CO through different polymers as the membrane material [40–43], it is known that CO transport behavior is similar to that of N_2 [44]. Nevertheless, almost all of the trade-off plots described in literature like Figure 1 are for pure gases (pure polymers; 35 °C). While Robeson plots are a useful screening tool for new materials, new features to assess the real performance of gas mixtures through conventional glassy polymers are required if the objective is to determine the feasibility of the membrane process for a specific industrial application [45].

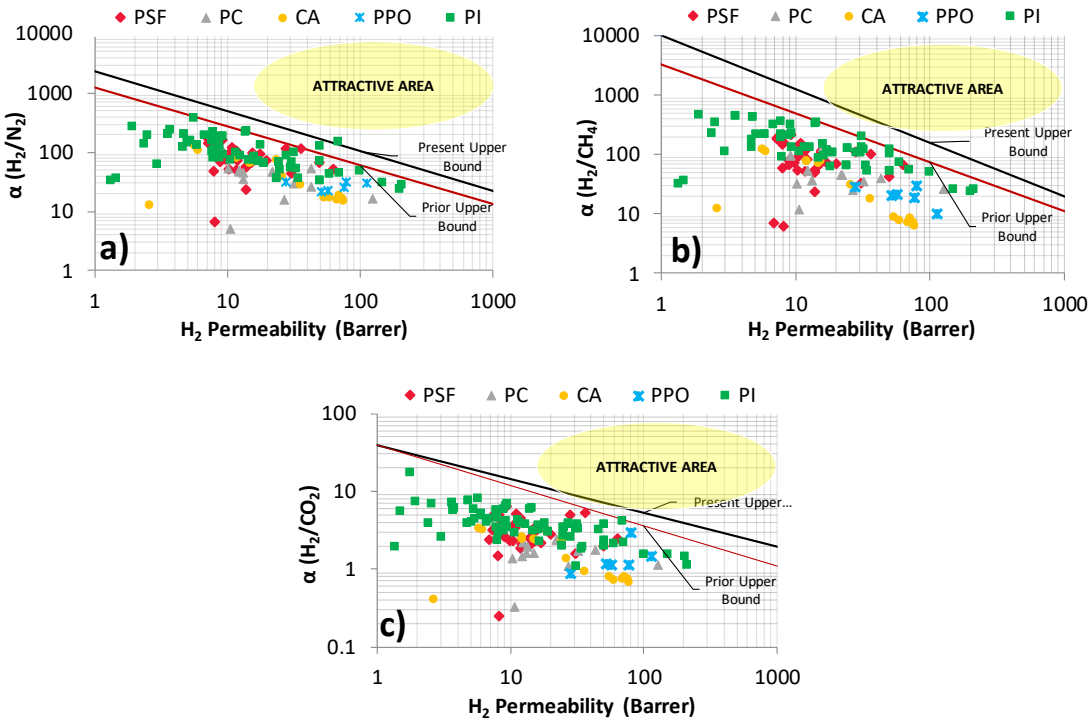

Figure 1. Comparison on desired selectivity and permeability for commercially available DPMs for a) H_2/N_2 separation, b) H_2/CH_4 separation and c) H_2/CO_2 separation. ♦ PSF: Polysulfones; ▲PC: Polycarbonates; ● CA: Cellulose acetate; ⨯ PPO: Polyphenyloxide; ■ PI: Polyimide

The Robeson upper - bound limits were included for each gas pair showing the performance improvement compared to those that were published in 1991; however, most of the polymeric membranes fabricated from commercial available polymers are still distant from the highlighted attractive area [46,47]. As it is illustrated, PIs constitute the largest group by far for hydrogen enrichment. As for hydrogen-selective DPMs, H_2 and CO_2 permeabilities fluctuated between 2.4 to 125 and 0.6 to 84.6 Barrer, respectively, resulting in H_2/CO_2 theoretical selectivities of 1.5 to 5.9. Due to their high hydrogen selectivity with respect to CO_2, N_2, CH_4 and CO, in order to obtain the maximum hydrogen purity to meet the quality standards of fuel cells, we decided to study the permeation behavior of the three commercial DPMs summarized in Table 2. In all three cases the membranes have been supplied as homogeneous dense films by the suppliers and were used without further modification. Membrane thicknesses were measured using a digital micrometer Mitutoyo Digmatic Series 369 (accuracy ± 0.001 mm). For each membrane, five repetitions were made at different points along the organic material, where average values and standard deviations were obtained. The membrane thicknesses for polyetherimide (PEI), polyethersulfone (PES) and polybenzimidazole (PBI) were determined to be 27.4 ± 1.1, 29.2 ± 1.1 and 58.4 ± 0.5 μm, respectively. Although relatively thick membranes were used, the main objective of this work has been

to evaluate the permeabilities for different components of gas mixtures. Since the permeabilities are assumed to be independent of the membrane thickness, the information obtained in this work is expected to be useful as a criterion for selecting the most suitable membrane material for a given separation. These materials should be further processed in the form of anisotropic membranes with a thin selective dense layer.

Table 2. Properties of the commercial studied H_2-selective membranes

Brand Names	Short name	Supplier	T_g (°C)	ρ (g cm^{-3})
ULTEM® 1000B	PEI	GoodFellow from SABIC	217	1.27
Ultrason® E	PES	GoodFellow from BASF	222	1.37
Celazole®	PBI	PBI Performance Products	427	1.30

2.3. Permeation set-up

In lab-scale experiments, commercial flat hydrogen selective membranes based on polymers were tested in order to separate multicomponent gas mixtures. A schematic illustration of the set-up indicating the coupled equipment is presented in Figure 2. The permeation set-up confers the possibility of performing pure and mixed gas permeation experiments, at predetermined gas concentrations and flow rate levels. All gases in this study had purities higher than 99.9 % and were supplied by Air Liquide.

Henceforth, gas separation experiments were carried out by means of multicomponent mixed gas separation tests using a continuous flow permeation cell. The membrane module consists of two stainless steel 316 cylindrical chambers pressed onto each other, with retentate volume of 50.9 cm^3 (9 cm ID x 0.8 cm upstream height). The polymeric films have been placed on a porous metallic plate (Mott Corp. US, 8.9 cm OD x 0.5 cm W, media grade 20, 316L stainless steel) and sealed by Kalrez® O-rings (9 cm ID x 0.4 cm W). The studied membranes are cut off from the dried polymeric film in circular shape and after the insertion in the permeation cell, it results an effective membrane area of 55.4 cm^2. The feed and sweep gas flowrates were controlled using Bronkhorst digital mass flow controllers' series F-201CV (0−0.1 L_N min^{-1}) for all gases, except for H_2 that was F-201CV (0−0.2 L_N min^{-1}). The gas permeates through the membrane material and after it is removed by a sweep gas (Helium). Two pressure transducers, from Ashcroft series GC-35 (0 – 8 bar) followed by a needle valve and placed at each side of the membrane, are used to set the transmembrane pressure for the separation according to the experimental design.

The membrane testing apparatus is placed in a thermostatic chamber (Memmert Excel) to ensure isothermal operation and an additional thermocouple was placed in order to control the input temperature of the gases. The composition of permeate and retentate streams was real-time analyzed by gas chromatography (Tracera GC-2010) equipped with a Barrier Ionization Discharge (BID) detector of ppb quantity level. The GC is suited with two columns, 1) molecular sieve capillary column (SH/Rt®/Msieve 5A) for H_2, N_2 , CO, and CH_4 separation and 2) fused silica capillary column (Carboxen® 1010 Plot) for CO_2 separation. The total acquisition time of the proposed gas chromatographic methods for analyzing the permeate and retentate streams was 9 minutes. Helium is employed as the carrier gas in both columns with a constant pressure of 4.5 bar.

Before starting a series of experiments, a vacuum pump was used to evacuate the whole permeation setup from undesired species and purge on the low pressure side of the equipment. The permeate side was kept under slightly higher ambient conditions ($p^P \approx$ 0.1 barg) to detect leaks by pressure decay. Constant steady-state values of retentate and permeate flux and composition were reached in less than 2 h. During this period the composition of the permeate stream was continuously analyzed, while the retentate was analyzed at least three times. Thus, once the constant steady-state is reached, the permeability of gases for each test is assessed using at least the last three injections, whose relative standard deviation (RSD) for peak area was not more than 1.5 %, showing high repeatability for the proposed gas chromatographic methods.

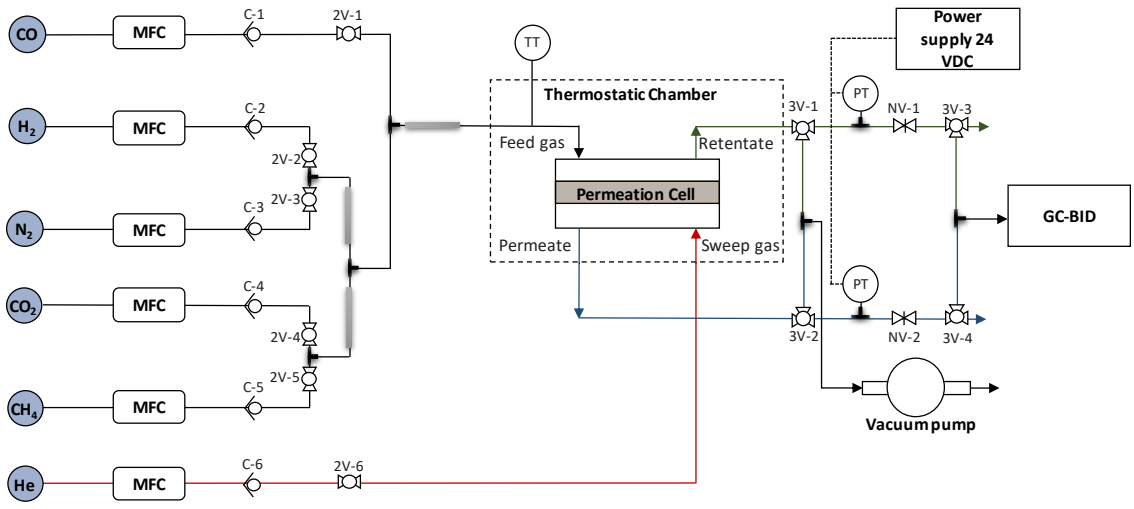

Figure 2. Mixed-gas permeation set-up. MFC, flow controller; C, check valve; 2V, 2-way valve; 3V, 3-way valve; TT, thermocouple; PT, pressure transducer; NV, Needle valve; GC-BID, gas analyzer. Feed gas (black); Sweep gas (red); Permeate (blue); Retentate (green).

A series of experiments was carried out to assess permeation and separation properties of the membranes. The process variables examined were the operation temperature, feed pressure, and the inlet gas composition described above in Table 1. When steady state transmembrane flux was reached, and the feed flow rate was much greater than the gas flux through the polymer film (i.e. stage cut < 0.5 %), Eq. (1) was used to evaluate permeabilities. The chosen flowrate conditions were set to guarantee that no significant polarization phenomena occur in the fluid phases adjacent to the membrane. When the same membrane was used for several tests, the experimental runs were conducted in the order of increasing CO_2 content in the inlet gas composition as follows: APG (H_2/ N_2/ CH_4 (% vol.): 58.6/ 25.7/ 15.7) , then COG (H_2/ N_2/ CO_2/ CO/ CH_4 (% vol.): 60.2/ 4.7/ 2.1/ 6.8/ 26.2) and MPG (H_2/ N_2/ CO_2/ CO/ CH_4 (% vol.): 63.1/ 11.3/ 11.1/ 3.4/ 11.2). The design boundaries for temperature were selected in the range of 25 to 45 °C, since the industrial gaseous waste streams under study are usually released to the air at room temperature. Beyond temperature and gas composition, the upstream pressure effect was also studied in the range of 4 to 7 barg. To sum up, the impact of the process variables on the real membrane performance was investigated, at the conditions given in Table 3.

Table 3. Operating experimental conditions for mixed gas experiments

Constant parameters	**Value**
Feed gas flowrate, Q_i^F (cm^3 (STP) min^{-1})	75
Sweep gas flowrate, Q^S (cm^3 (STP) min^{-1})	7 - 15
Effective area, A (cm^2)	55.4
Variable parameters	**Value**
Temperature, T (°C)	25/35/45
Upstream pressure, p^F(barg)	4/5.5/7
Feed gas composition, x_i^F (%vol.)	APG/COG/MPG

3. RESULTS AND DISCUSSION

This section shows the main results obtained by investigating the permeation of pure gases and multicomponent gas mixtures of H_2, N_2, CH_4, CO, and CO_2 through dense polymeric films. Also, using experimental results of mixed gas separations, permeability has been evaluated as a function of temperature, pressure and feed concentration.

3.1. Pure gas experiments

First, single gas permeation experiments were performed to obtain and compare permeability coefficients with literature data and also to have a benchmark for the multicomponent gas experiments. Table 4 shows the permeability data of pure gases for three DPMs: PEI, PES and PBI, in addition to values reported in literature. The pure-gas measurements were conducted at a constant temperature of 35°C and a transmembrane pressure difference of 3.5 to 5.5 bar, until constant steady-state values of permeate flux and composition. The permeability error is determined by the membrane thickness standard deviation and each membrane sample was measured in two replicates.

Based on the permeability values determined, it was revealed that the membranes allowed the gases to permeate in the following order: H_2 >> CO_2 > N_2 ≈ CO ≈ CH_4, where this phenomenon represents the hydrogen-selective characteristic of the membranes. It was noticeable that H_2 permeability was always higher than CO_2 permeability for all the membranes, and correlates with the kinetic diameter of the gases with H_2 as the smallest one (2.89 Å) compared to CO_2 with bigger size (3.3 Å), and then follow by N_2 (3.64 Å), CO (3.76 Å) and CH_4 (3.8 Å). The kinetic diameters are not only related to the gas molecular size, but also to their molecular structure [32]. H_2 is a small and non-condensable gas so that it can easily permeate through the membranes unlike the other pure gases.

According to the obtained values, the performance results for the given membranes showed two different ranges of permeability coefficients, which values agree with similar studies in literature. Consequently, H_2 permeabilities obtained with PEI and PES membranes that fluctuated between P_{H_2}= 8 to 12 Barrer at 35 °C, are 10 times higher than those obtained with PBI membrane at the same conditions, which ranged from P_{H_2}= 0.5 to 0.8 Barrer. This is possibly related to the polymers' chemical and physical properties. It was known that PBI-based materials exhibit higher density (1.3 g cm^{-3}) than other glassy polymers (PEI: 1.27 g cm^{-3}, PSF: 1.24 g cm^{-3}, etc.), which renders low flexibility and rigid chain-packing structure [48]. Thus, the immobilization of the polymer matrix would result in lesser free volume for gas diffusion, which finally presented lower permeability.

Considering first the PEI membrane, it presents an average permeabilities (Barrer): P_{H_2}= 8.4 ± 0.4, P_{CO_2}= 2.1 ± 0.1, P_{N_2}= 0.03 ± 0.002, P_{CH_4}= 0.50 ± 0.003 and P_{CO}= 0.40 ± 0.002, values obtained at 35 °C in a narrow range of pressures (3.5 - 5.5 bar). Other reported samples of PEI show similar H_2 permeabilities; i.e., P_{H_2}= 7.8 Barrer at 30 °C [49] and P_{H_2}= 6.9 Barrer at 35 °C [50]. For this material, CO_2 permeabilities also are in

agreement with similar studies in literature; i.e., P_{CO_2}= 1.3 Barrer at 30 °C [49] and P_{CO_2}= 2.4 Barrer at 25 °C [51]. On the other hand, permeability coefficients of PES membrane are (Barrer): P_{H_2}= 11.2 ± 0.4, P_{CO_2}= 4.4 ± 0.2, P_{N_2}= 0.08 ± 0.01 , P_{CH_4}= 0.20 ± 0.01 and P_{CO}= 0.11 ± 0.01, at average conditions (35 °C and 3.5 - 5.5 bar). Other samples of this material in literature show relatively lower H_2 permeabilities; i.e., P_{H_2}= 5.8 Barrer at 25 °C [52] and P_{H_2}= 9.0 Barrer at 35 °C [53], which can be ascribed to the difference of commercial materials used. In contrast, PBI-based materials exhibit the lowest permeability coefficients (Barrer): P_{H_2}= 0.6 ± 0.1, P_{CO_2}= 0.3, P_{N_2}= 0.002, P_{CH_4}= 0.001 and P_{CO}= 0.004, at average conditions. The obtained results are consistent with those of older studies at similar conditions; i.e., P_{H_2}= 0.5 - 0.6 Barrer at ca. 30 °C [48,54]. However, previously reported values of CO_2 permeabilities are slightly lower in comparison with those reported in this work; i.e., P_{CO_2}= 0.22 Barrer at 23 °C [54] and P_{CO_2}= 0.16 Barrer at 35 °C [48]. Consequently, H_2/CO_2 selectivity for PBI membrane, which ranges between α_{H_2/CO_2}= 2 – 3, is slightly lower than the ideal values obtained from the literature. In general terms, it can be observed that the selected membranes provide H_2 permeability and ideal selectivity values well-agreed with the previously reported data in the literature for other PEI, PES and PBI membranes. However, it must be pointed out that H_2/CO_2 selectivities are slightly lower than the ideal values obtained from the literature regardless of the membrane used. Nevertheless, H_2/N_2 and H_2/CH_4 selectivities are higher to a certain extent that those previously reported. The differences observed can be partially attributed to the fact that some results reported in literature have been obtained by the traditional time-lag technique. In addition, no previous data of the given membranes have been reported regarding CO, thus the obtained values constitute original data for these polymeric materials.

3.2. Mixed gas experiments

In this analysis, the impact of operating conditions (temperature, pressure and inlet mixed-gas composition) over permeability, selectivity and outlet gas purity was studied for each membrane. For synthetic gas mixtures based on real industrial hydrogen-rich waste gases, the performance of three DPMs: PEI, PES and PBI, was characterized to assess the appropriateness of the each membrane for a given separation task.

376

Table 4. Pure gas permeation properties of different polymeric membranes

		Permeability (Barrer)						Ideal selectivity				Polymer properties			Operating conditions		
Membrane	Membrane type	H_2	He	CO_2	N_2	CH_4	CO	H_2/CO_2	H_2/N_2	H_2/CH_4	H_2/CO	T_g (°C)	ρ (g cm^{-3})	δ_N (μm)	T (°C)	Δp (bar)	Ref.
PEI	**ULTEM® 1000B**	**7.9 ± 0.3**	**-**	**2.1 ± 0.1**	**0.03± 0.001**	**0.05 ± 0.002**	**0.04 ± 0.002**	**3.7**	**281**	**155**	**196**	**217**	**1.27**	**25**	**35**	**5.5**	**This work**
		8.9 ± 0.5	**-**	**2.2 ± 0.1**	**0.03± 0.002**	**0.05 ± 0.003**	**0.04 ± 0.002**	**4.1**	**330**	**168**	**223**	**217**	**1.27**	**25**	**35**	**3.5**	
	ULTEM® 1010	-	8.80	1.5	0.05	0.04	-	5.9	163.0	220.0	-	215	-	-	35	3.5	[55]
	ULTEM® XH6050	-	9.40	1.3	0.05	0.04	-	7.1	184.3	261.1	-	-	1.27	-	35	10 (3.5 H_2)	[56]
	-	7.8	-	1.3	0.05	0.04	-	5.9	166.0	222.9	-	215	-	-	30	-	[49]
	ULTEM® 1000	-	-	-	0.05	-	-	-	-	-	-	218	1.27	25	35	10	[57]
	-	-	-	1.3	-	0.04	-	-	-	-	-	215	1.28	-	35	10	[58]
	ULTEM® 1000	-	-	2.4	-	0.09	-	-	-	-	-	214	1.26	-	25	10	[51]
	ULTEM® 1000	6.9	-	1.6	0.05	0.03		4.4	133	238	-	215	-	-	35	5	[50]
PES	**Ultrason® E**	**10.5 ± 0.4**	**-**	**5.6 ± 0.2**	**0.08± 0.003**	**0.2 ± 0.01**	**0.11 ± 0.004**	**1.9**	**131**	**52**	**95**	**222**	**1.37**	**25**	**35**	**5.5**	**This work**
		12.0 ± 0.5	**-**	**3.1 ± 0.1**	**0.09± 0.01**	**0.2 ± 0.01**	**0.11 ± 0.01**	**3.8**	**130**	**58**	**106**	**222**	**1.37**	**25**	**35**	**3.5**	
	Radel® A	-	-	3.2	0.07	0.10	-	-	-	-	-	-	-	HF	RT	1.36 –13.6	[59]
	Radel® A - 300	5.8	7.6	-	0.10	-	-	-	73.7	-	-	-	-	film	25	10	[52]
	Radel® A	9.0	9.1	3.4	0.13	0.11	-	2.7	70.0	82.7	-	-	-	60-70	35	2-35	[53]
	Radel® A	9.0	9.1	3.4	0.13	0.11	-	2.7	70.6	81.3	-	-	-	-	35	10 (2 H_2/He)	[60]
PBI	**Celazole®**	**0.52 ± 0.004**	**-**	**0.3 ± 0.2**	**0.002±0**	**0.001±0**	**0.004±0**	**2.0**	**260**	**> 400**	**130**	**427**	**1.30**	**55**	**35**	**5.5**	**This work**
		0.77 ± 0.02	**-**	**0.3 ± 0.2**	**0.002±0**	**0.001±0**	**0.004±0**	**3.0**	**198**	**> 400**	**198**	**427**	**1.30**	**55**	**35**	**3.5**	
	Celazole®	0.53	-	0.22	0.016	-	-	2.4	33.7	-	-	427	1.30	-	23	20	[54]
	Celazole®	1.74	-	0.88	0.063	-	-	2.0	27.9	-	-	427	1.30	-	80	20	[54]
	Tailor-made	0.6	1.05	0.16	0.005	0.002	-	3.8	125	333.3	-	416	1.33	40	35	20	[48]
	Tailor-made	76.8	-	3.33	0.78	-	-	23.0	98.3	-	-		1.37		250	1.5 – 3.5	[61]

377

3.2.1. Temperature effect on mixed-gas permeation

The temperature effect on gas permeability through the DPMs was studied over a temperature range of 25 to 45 °C for the different synthetic waste gas streams, at $\Delta p \approx$ 5.5 bar. As it is illustrated in Figure 3, all gas permeabilities were increased at higher temperatures. Generally, for DPMs, the temperature affects the energies of the gas molecules as well as the mobility of the polymeric chains of the membrane. Thus, a temperature increment in the membrane changes the flexibility of the polymeric chains, which improves the gas motion through the membrane [62,63].

As it is represented in Figure 4 and regardless of the DPM used, all studied cases H_2/N_2, H_2/CH_4 and H_2/CO selectivity values decrease with temperature, while H_2/CO_2 increases. These results are in agreement with previous studies [43,64]. This behavior can be attributed to the changes of the transport and thermodynamic properties (i.e. diffusion and solubility) of specific gases included in the mixed gas mixtures, with raising the temperature. Theoretically, elevating the temperature enhances gas diffusion, while on the other hand, reduces solubility in a significant manner. In the case of CO_2, as the temperature increased the regime was shifted from diffusion-limited to sorption-limited because of the higher dependence of diffusivity on temperature. Thus, increasing rate of CO_2 permeability with temperature was lower than the increasing rate of H_2 and therefore the H_2/CO_2 selectivity increased [43,64].

Also, in Figure 4 it can be seen that the achievable H_2/CO_2 selectivity of PEI membrane increased from 3.9 at 25 °C to 4.9 at 45 °C using COG, while this increase is less pronounced using MPG from 3.6 at 25 °C to 3.8 at 45 °C. This behavior is also observed with PES membrane, thus, raising the temperature the H_2/CO_2 selectivity values enhanced from 1.7 at 25 °C to 2.1 at 45 °C using COG, whereas the performance improvement is less evident using MPG, varying from 1.4 at 25 °C to 1.6 at 45 °C. However, mixed gas permeability results from PBI membrane lead to slightly higher CO_2 permeability values than those of hydrogen, showing a non-hydrogen-selective behavior at the temperature range under study.

Figure 4 shows that the H_2/CO_2 selectivity for PEI membrane decays from α_{H_2/CO_2}= 4.2 using COG, to α_{H_2/CO_2}= 3.8 using MPG, in accordance with findings reported in literature [55]. Thus, strong dependency of H_2 permeability on CO_2 concentration inducing this gas in a decay of H_2/CO_2 selectivity in mixed-gas experiments. This H_2/CO_2 selectivity decay is also observed for PES membrane, where it decreases from α_{H_2/CO_2}=

411 2.0 using COG, to α_{H_2/CO_2}= 1.5 using MPG, which is a similar trend as reported by Yong
412 et al. [65].

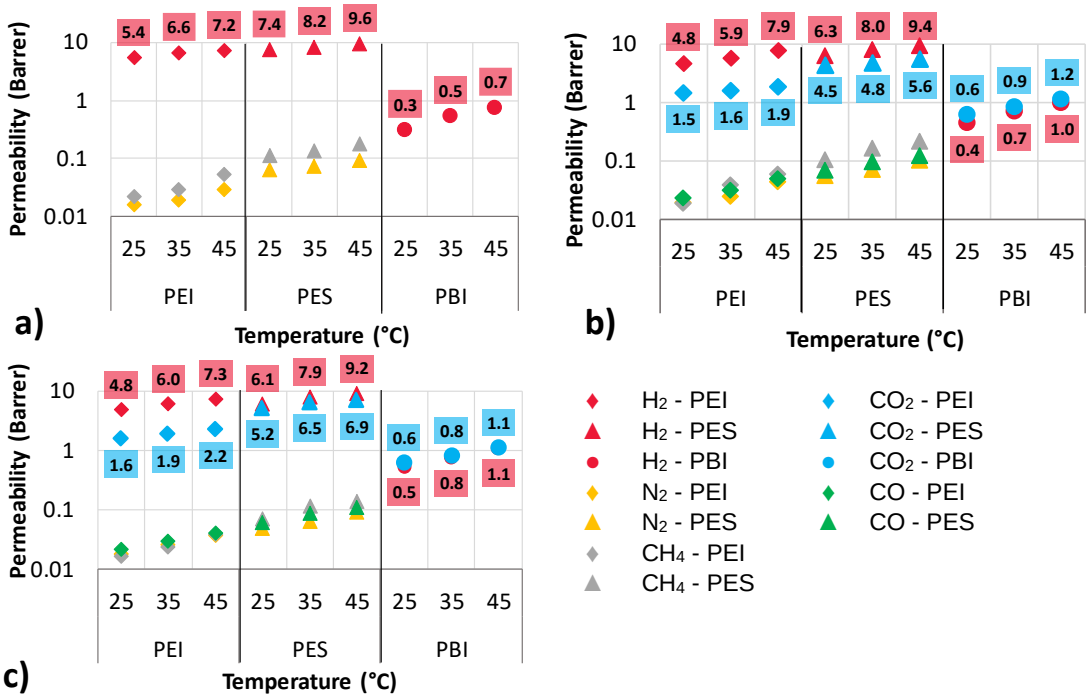

413 Figure 3. Temperature effect of mixed-gas permeabilities, measured at $\Delta p \approx 5.5$ bar: a) APG, b)
414 COG and c) MPG

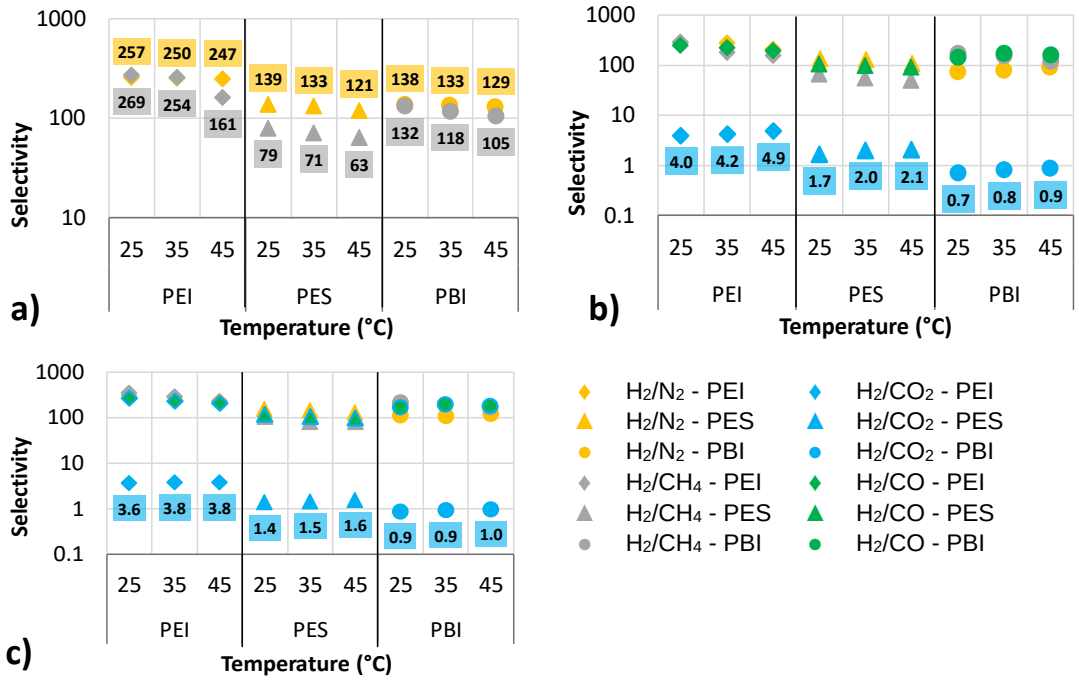

415 Figure 4. Temperature effect of mixed-gas selectivities, measured at $\Delta p \approx 5.5$ bar: a) APG, b)
416 COG and c) MPG

417 Furthermore, in order to explore the dependency of the gas permeability on
418 temperature, the data were correlated with an Arrhenius-type equation:

$$P_{\mathrm{i}} = P_0 \cdot e^{\left(-\frac{E_p}{RT}\right)} \quad \text{Eq. (3)}$$

with P_0 as the pre-exponential factor, E_p as the permeation activation energy, T as the temperature and R as the ideal gas constant (8.314 J mol^{-1} K^{-1}). E_p values for the transport of each gas through each membrane were obtained from the slope of permeability (in logarithmic form) versus the reciprocal temperature. Fitting experimental permeability data to Eq. (3) showed high coefficients of determination for the Arrhenius parameters (R^2 > 0.9 in all cases, with R^2 > 0.95 in the vast majority of cases). The specific E_p parameters at $\Delta p \approx 5.5$ bar for permeation of H_2, N_2, CH_4, CO and CO_2 are summarized in Table 5. The permeation activation energy increased in the order CO_2 <H_2 <CO <N_2 <CH_4, , in the case of PEI and PES membranes, which is the same tendency as reported in other glassy polymeric membranes [66,67]. These glassy polymers present high values for the activation energy of permeation for CH_4, N_2 and CO, and therefore, the permeability coefficients strongly depend on temperature. The dependency on temperature for hydrogen as the smallest of the gases is much weaker. On the other hand, CO_2 shows the lowest E_p value among the gases considered, likely in view of the larger contribution of sorption, an exothermic process, to the permeation mechanism [43,68]. On the other hand, it is well known that PBIs have very rigid, well-packed structures due to their strong intermolecular interactions, resulting in very low gas permeation properties; a moderate increase in temperature produces an appreciable change in polymer backbone chain flexibility, leading to an increase in gas permeability. The higher sensitivity of the PBI polymer to changes in temperature lead to energy activation values for this polymer that are higher compared to the other two polymers studied.

Table 5. Activation energy of H_2, N_2, CH_4, CO and CO_2 permeation through DPMs

		E_p (kJ mol^{-1})				
Membrane	**Mixed gas**	**H_2**	**N_2**	**CH_4**	**CO**	**CO_2**
PEI	APG	11.5	22.5	34.3	-	-
	COG	19.5	31.4	44.1	28.2	8.9
	MPG	16.4	28.0	33.1	25.2	13.4
PES	APG	9.9	15.3	18.5	-	-
	COG	15.1	23.4	28.3	21.3	8.6
	MPG	15.5	23.9	25.8	21.9	11.1
PBI	APG	32.1	34.7	41.0	-	-
	COG	23.0	22.4	38.2	29.7	18.7
	MPG	28.2	26.4	38.8	25.8	23.2

3.2.2. Pressure effect on mixed-gas permeation

The permeability coefficients of each gas were also measured as a function of the upstream feed pressure ranging from 4 to 7 barg for each synthetic waste gas stream and membrane material, and at 35 °C. Furthermore, the permeate side was kept under slightly higher atmospheric pressure.

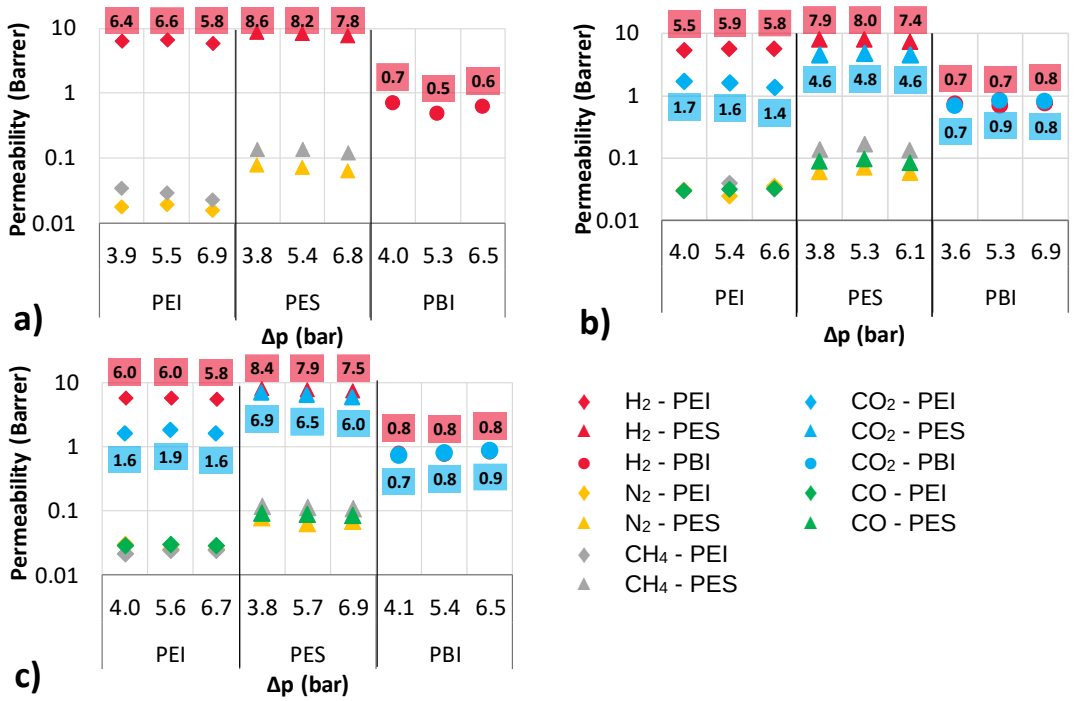

Figure 5. Pressure effect of mixed-gas permeabilities, measured at 35 °C: a) APG, b) COG and c) MPG

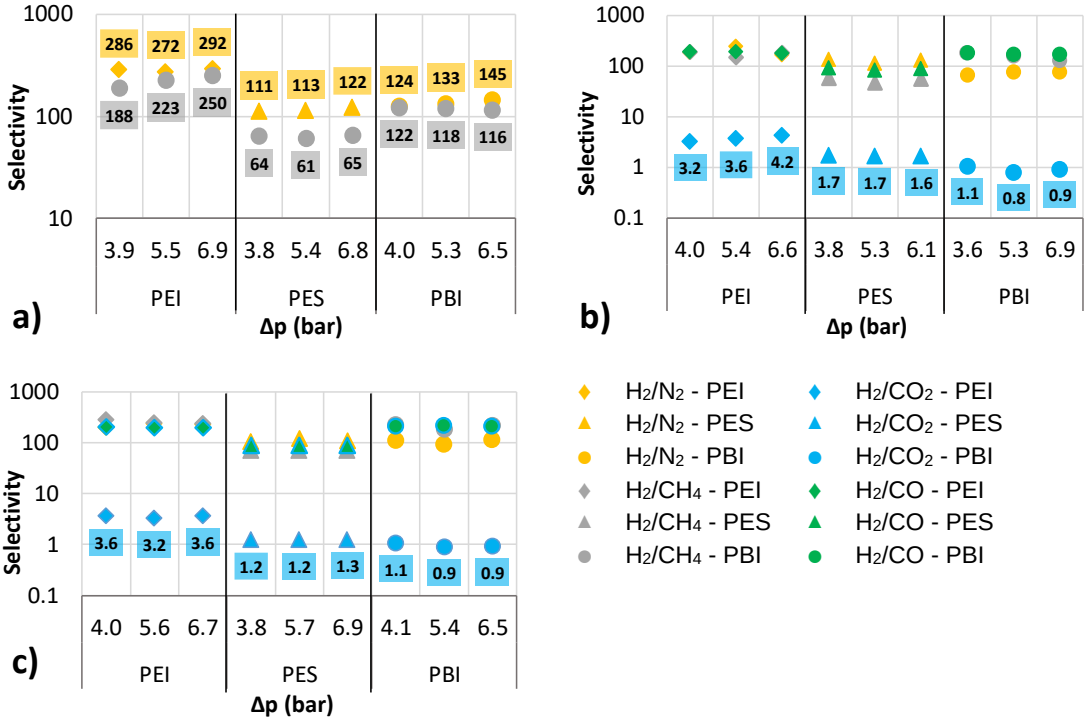

Figure 6. Pressure effect of mixed-gas selectivities, measured at 35 °C: a) APG, b) COG and c) MPG

The permeability of mixed gases through the DPMs, as a function of the transmembrane pressure difference, is shown in Figure 6. Upon increasing the applied pressure, the permeability of low-sorbing penetrants (i.e. H_2, N_2, CH_4, CO) as feed gas exhibit non-significant change with pressure (< 15 % deviations), although a slight decrease can be intuited. This is a classical behavior in glassy polymeric membranes, where the transport is more diffusion dependent for less soluble penetrants. Initially, diffusion increases with applied pressure. However, the compaction effect leads to less diffusion rate of low-sorbing gases, which causes the permeability to decrease with pressure [69,70]. Meanwhile the permeability tendency observed for CO_2 showed a decreasing trend when the transmembrane pressure increased. The decrease is related to the interaction of CO_2 molecules with the polymer matrix, and according to the dual-sorption model, the Langmuir sorption sites become saturated with gas molecules [63,71].

3.2.3. Comparing membrane performances

Experiments with multicomponent gas mixtures of H_2, N_2, CH_4, CO and CO_2 were performed. Generally, the permeation behavior of a pure gas through a membrane depends mainly on the properties of the gas and membrane as well as the operating conditions. As for gas mixtures the transport behavior of one component through the membrane is affected by the presence of other penetrants so that it deviates from that of the pure gas [43]. The deviations are in general attributed to different factors, from which the solubility coupling by competitive sorption effects and membrane plasticization by CO_2 are more prevalent (assuming that in our case the concentration polarization phenomena are not significant). Figure 7 shows the Robeson's trade-off lines between the selectivity and permeability for H_2/N_2, H_2/CH_4 and H_2/CO_2.

Although single gas permeabilities are similar to those reported in previous research, competitive sorption effect results in a slight drop in the permeability of H_2 with respect to pure gases using PEI and PES membranes. This effect was ascribed to the fact that the permeability of gases in mixed gas experiments is overall affected by the presence of CO_2 in the mixture of gases [55,65]. As a matter of fact, these interactions depend on several factors, such as the number of components in the mixture, type of components and operating parameters [72]. However, mixed-gas experimental results using PBI membrane showed higher H_2 permeabilities than pure gas tests, as it has been observed by other authors in literature [61].

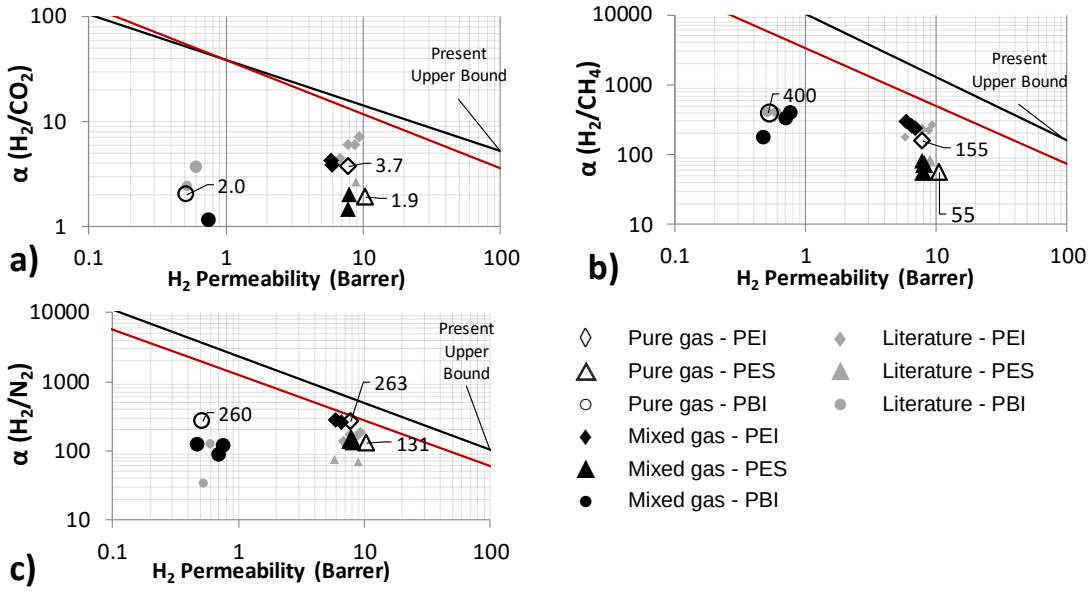

Figure 7. Separation performance with single and mixed gases, measured at 35 °C and $\Delta p \approx$ 5.5 bar: a) H_2/N_2, b) H_2/CH_4 and c) H_2/CO_2

For all the studied membranes, there is no coupling or competitive sorption between H_2 and N_2, CO and CH_4, with slight deviations between ideal and mixed-gas selectivity values of less than 4.7 % in PES, 11.2 % in PEI and 15.0% in PBI. Light gases (i.e. H_2, N_2) with very low solubility in polymer materials, they only weakly affect the property and behavior for polymers, and do not influence the mutual diffusion and solubility parameters in the process of simultaneous transport of gases in the separation of the mixture.

Nevertheless, the experimental results implied that the growing presence of CO_2 in the feed gas mixture caused difficulties in the whole separation process, due to the fact that this high-sorbing gas can fairly be dissolved in the membrane. For heavy gases (i.e. CO_2) with high solubility, the applicability of ideal permeation parameters implies higher uncertainty in predicting permeation results [33]. According to these results, although the DPMs do not cross the upper bound established in 2008, most of the membranes under study lay close to the upper bound found previously, in 1991.

3.2.4. Gas composition effect on hydrogen purity

Besides the above-mentioned variables, the inlet gas composition of the mixture to be separated is another factor that affects the overall performance of the membrane. Thus, tertiary and quinary mixed-gas experiments ($H_2/N_2/CH_4/CO/CO_2$) were performed

by applying three different inlet gas compositions based on industrial waste gas streams (APG, COG and MPG), where hydrogen content is *ca.* 60 %. As might be expected because of permeability and selectivity values obtained, PEI membrane attained the highest hydrogen gas purities, followed by PES and PBI membranes.

Based on Figure 8, after permeation using PEI membrane at the given conditions (cell dimensions, flowrates at low stage cut, operating parameters), hydrogen in permeate reached up to 99.7 % vol. H_2 from APG, 98.8 % from COG and 95.4 % from MPG. Then, the product purity drops using PES membrane down to 99.2 % vol. H_2 from APG, 97.0 % from COG and 89.3 % from MPG. Regarding PBI membrane, the hydrogen purities are quite similar to those obtained using PES, as 99.4 % vol. H_2 from APG and 96.1 % from COG, whereas the purity value decays down to 86.6 % when MPG is used as feed gas stream.

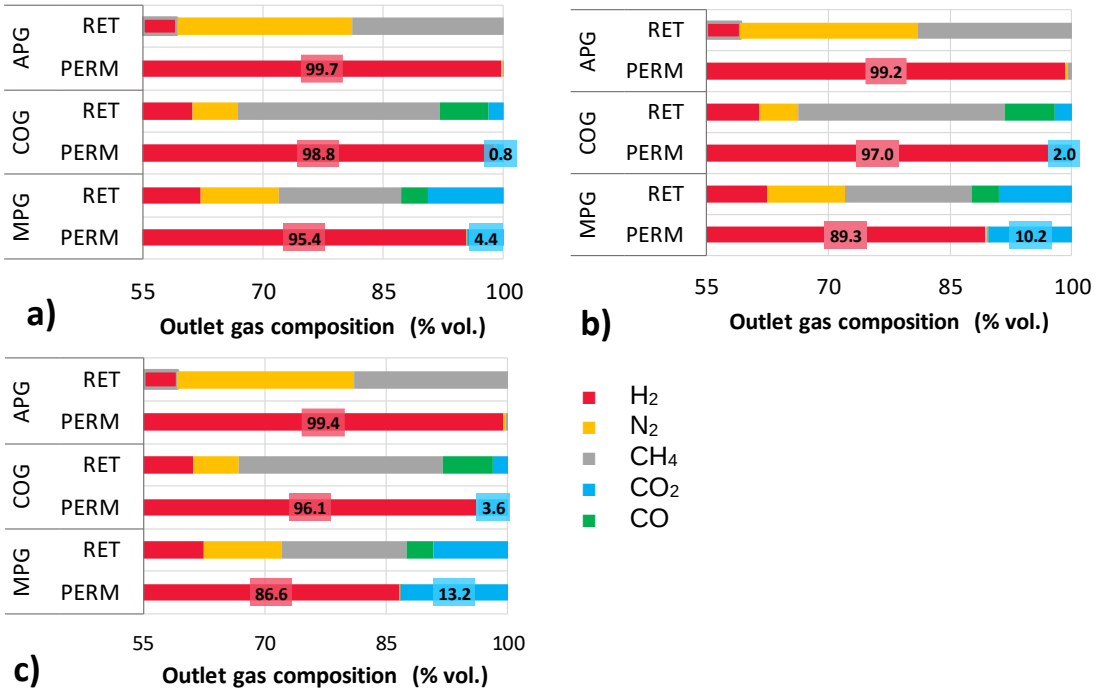

Figure 8. Composition of retentate (RET) and permeate (PERM) streams as function of feed gas, measured at 35 °C and $\Delta p \approx 5.5$ bar. a) PEI, b) PES and c) PBI membranes

Regardless the DPMs studied, the purification yield was slightly lower using MPG as feed gas, possibly due to the existence of higher CO_2 content in the inlet stream. Thus, hydrogen purity is strongly affected by the CO_2 feed concentration, while the results showed that hydrogen purity remains almost constant to temperature and pressure changes in these ranges. This implies that the enrichment degree of hydrogen as the fastest gas penetrant was considerably dependent on the amount of carbon dioxide in

the feed gas. The experimental results implied that the growing amount of carbon dioxide present in the feed gas caused a decrease in the enriched hydrogen permeate stream.

Even though these results are still far from the quality requirements to feed fuel cells (> 99.9 %), they give relevant knowledge on membrane hydrogen purification yield to the scientific community, as the first upgrading step before further purification. In consequence with the results of state-of-the-art membranes studied in flat sheet form, PEI membrane achieve the highest purity of hydrogen, while simultaneously showed higher permeability and H_2/CO_2 selectivity. Although the maximum hydrogen purity obtained using PEI membrane was 99.7 % vol. H_2 from APG, 98.8 % from COG and 95.4 % from MPG, it would be necessary further upgrading to meet fuel cell quality standards. This could be done through the use of cascade membrane module systems or coupling it with conventional processes, such as hybrid membrane-PSA systems. The configuration and operation of a hybrid systemcould be designed and optimized using process flow sheet simulation packages to achieve optimal results.

4. CONCLUSIONS

This work reports new data on the performance of commercial polymer-based membranes for hydrogen selective separations, which serves as the basis for the evaluation of the membrane technologies for hydrogen recovery from industrial waste gases. The permeation of pure gases and multicomponent mixtures of H_2, N_2, CH_4, CO, and CO_2 at different operating conditions through dense polymeric films has been investigated. Moreover, operating conditions that govern the practical feasibility of different membranes are discussed. In this way, new knowledge on membrane behavior related to real process conditions is revealed for commercially available polymeric membranes. This work renders valuable insights into the status of a membrane-based processes for hydrogen recovery applicable to industrial waste gas streams.

Furthermore, the effect of process parameters on the performance of hydrogen-selective polymeric membranes was investigated. In this paper, mixed-gas permeation through three different non-porous polymeric membranes (PEI, PES, PBI) has been studied over three different synthetic waste gas streams (COG, APG and MPG). Also, the influence of temperature, transmembrane pressure difference and feed gas composition on gas permeation was examined. The major findings of this study are as follows;

- In the mixed gas system, all gas permeabilities were increased when increasing temperature. Even so, H_2/N_2, H_2/CH_4 and H_2/CO selectivity values decrease with temperature, while H_2/CO_2 selectivity increases.
- Permeability of low-sorbing penetrants (i.e. H_2, N_2, CH_4, CO) as feed gas exhibit insignificant change with pressure, whereas the permeability tendency observed for CO_2 showed a decreasing trend upon increasing the transmembrane pressure.
- Strong dependency of H_2 permeability on CO_2 concentration inducing this gas a decay of H_2/CO_2 selectivity in mixed-gas experiments for the studied membranes.
- Competitive sorption effect results in a drop in the permeability of H_2 with respect the pure gases using PEI and PES membranes, meanwhile the opposite effect was observe using PBI membrane.

In addition, with the experimentally obtained permeances, the required membrane area for a specific separation can be calculated and the optimum operating conditions can be found. Besides, membrane processes should be tested under real feeds to ensure membrane stability for long-term operation by evaluating trace components and extending the temperature and pressure ranges. Although the maximum hydrogen purity obtained using PEI membrane was 99.7 % vol. H_2 from APG, 98.8 % from COG and 95.4 % from MPG, it would be necessary further upgrading of the permeate stream to the required quality to comply with ISO 14687 series. This could be done through the use of cascade membrane module systems or a hybrid process that combines gas permeation with another conventional separation process, such as PSA.

ACKNOWLEDGMENTS

This research was supported by the projects CTQ2016-75158-R (AEI/FEDER, UE), RTI2018-093310-B-I00 (MINECO/AEI/FEDER, UE), and PEMFC-SUDOE project (SOE1/P1/E0293 - INTERREG SUDOE/FEDER, UE), “Energy Sustainability at the SUDOE Region: Red PEMFC-SUDOE”.

ABBREVIATIONS

APG	ammonia purge gas
BID	barrier ionization discharge
CA	cellulose acetate
COG	coke oven gas
DPM	dense, organic (polymeric) membranes

GC	gas chromatography
HF	hollow fibers
ICE	internal combustion engines
ID	inside diameter
ISO	International Organization for Standardization
MFC	flow controller
MPG	methanol purge gas
MSA	Membrane Society of Australasia database
NV	needle valve
OD	outside diameter
PBI	polybenzimidazole
PC	polycarbonate
PEI	polyetherimide
PEMFC	proton exchange membrane fuel cell
PERM	permeate stream
PES	polyethersulfone
PI	polyimide
PPO	polyphenyloxide
PSA	pressure swing adsorption
PSF	polysulfones
PT	pressure transducer
RET	retentate stream
RSD	relative standard deviation
RSD	relative standard deviation
RT	room temperature
STP	standard temperature (0 °C or 273 K) and pressure (1 atm)
TT	thermocouple
W	width

NOMENCLATURE

Parameters

x	mole fractions of component (% mol.)
E_p	permeation activation energy (kJ mol^{-1})
P_0	pre-exponential factor (Barrer)
P	gas permeability coefficient (Barrer)
Q	gas flow rate (cm^3 s^{-1})
T_g	glass transition temperature (°C)
p	pressure (barg)

Δp	pressure gradient across the membrane (bar)
A	area of the membrane (cm^2)
R	ideal gas constant ($J\ mol^{-1}\ K^{-1}$)
R^2	determination coefficient
T	operating temperature (°C)
δ	thickness of the membrane (cm)

Greek letters

$\propto_{i/j}$	selectivity of component i over component j
ρ	membrane density ($g\ cm^3$)

Subscripts/superscripts

F	feed
i, j	gas components
P	permeate
S	sweep gas

REFERENCES

[1] International Renewable Energy Agency (IRENA). Global energy transformation: A roadmap to 2050. www.irena.org. [accessed in 2019]

[2] Cherry RS. A hydrogen utopia? Int J Hydrogen Energy 2004;29:125–9.

[3] International Energy Agency (IEA). The future of hydrogen: Seizing today's opportunities 2019. www.iea.org. [accessed in 2019]

[4] Fraile D, Lanoix JC, Maio P, Rangel A, Torres A. CertifHy project. Overview of the market segmentation for hydrogen across potential customer groups, based on key application areas. 2015.

[5] Yáñez M, Ortiz A, Brunaud B, Grossmann IE, Ortiz I. Contribution of upcycling surplus hydrogen to design a sustainable supply chain: The case study of Northern Spain. Appl Energy 2018;231:777–87.

[6] ISO 14687: Hydrogen Fuel: Product Specification. Part 1: All applications except proton exchange membrane (PEM) fuel cell for road vehicles. 2009.

[7] ISO 14687: Hydrogen Fuel: Product Specification. Part 2: Proton exchange membrane (PEM) fuel cell applications for road vehicles 2009.

[8] ISO 14687: Hydrogen Fuel: Product Specification. Part 3: Proton exchange membrane (PEM) fuel cells applications for stationary appliances 2009.

[9] Ball, M., Wietschel M. The hydrogen economy: Opportunities and

challenges. New York: Cambridge University Press; 2009.

[10] Uehara I. Separation and purification of hydrogen. In: Ohta T, editor. Energy carriers and conversion systems, vol. 1., Paris: EOLSS; 2008, p. 268–82.

[11] Li P, Wang Z, Qiao Z, Liu Y, Cao X, Li W, et al. Recent developments in membranes for efficient hydrogen purification. J Memb Sci 2015;495:130–68.

[12] Ritter JA, Ebner AD. State-of-the-art adsorption and membrane separation processes for hydrogen production in the chemical and petrochemical industries. Sep Sci Technol 2007;42:1123–93.

[13] Conde JJ, Maroño M, Sánchez-Hervás JM. Pd-based membranes for hydrogen separation: Review of alloying elements and their influence on membrane properties. Sep Purif Rev 2017;46:152–77.

[14] Sanders DF, Smith ZP, Guo R, Robeson LM, McGrath JE, Paul DR, et al. Energy-efficient polymeric gas separation membranes for a sustainable future: A review. Polymer (Guildf) 2013;54:4729–61.

[15] Baker RW, Low BT. Gas separation membrane materials: A perspective. Macromolecules 2014;47:6999–7013.

[16] Liu K, Song C, Subramani V. Hydrogen and syngas production and purification technologies. Hoboken, NJ: Wiley-AIChE; 2009.

[17] Yin H, Yip ACK. A review on the production and purification of biomass-derived hydrogen using emerging membrane technologies. Catalysts 2017;7:297.

[18] Alique D, Martinez-Diaz D, Sanz R, Calles JA. Review of supported Pd-based membranes preparation by electroless plating for ultra-pure hydrogen production. Membranes (Basel) 2018;8:1–39.

[19] Bakonyi P, Nemestóthy N, Bélafi-Bakó K. Biohydrogen purification by membranes: An overview on the operational conditions affecting the performance of non-porous, polymeric and ionic liquid based gas separation membranes. Int J Hydrogen Energy 2013;38:9673–87.

[20] Koros WJ, Fleming GK. Membrane-based gas separation. J Memb Sci 1993;83:1–80.

[21] Wu F, Li L, Xu Z, Tan S, Zhang Z. Transport study of pure and mixed gases through PDMS membrane. Chem Eng J 2006;117:51–9.

[22] Dhingra SS, Marand E. Mixed gas transport study through polymeric membranes. J Memb Sci 1998;141:45–63.

[23] PRTR-España (Spanish Register of Emissions and Pollutant Sources). Environmental assessment (EA/ HU / 029) - Fertiberia, S.A. in Palos de la Frontera (Huelva). 2007.

[24] Sun Q, Liu J, Liu A, Guo X, Yang L, Zhang J. Experiment on the separation of tail gases of ammonia plant via continuous hydrates formation with TBAB. Int J Hydrogen Energy 2015;40:6358–64.

[25] Wu Z, Wenchuan W. The recovery of ammonia from purge gas. www.cryobridge.com/Ammonia.pdf. [accessed in 2017]

[26] Yáñez M, Relvas F, Ortiz A, Gorri D, Mendes A, Ortiz I. PSA purification of waste hydrogen from ammonia plants to fuel cell grade. Sep Purif Technol 2020; 240;116334.

[27] Agahzamin S, Mirvakili A, Rahimpour MR. Investigation and recovery of purge gas streams to enhance synthesis gas production in a mega methanol complex. J CO2 Util 2016;16:157–68.

[28] Arthur T. Control structure design for methanol process. Master thesis. Norwegian University of Science and Technology, Trondheim, 2010.

[29] Bermúdez JM, Arenillas A, Luque R, Menéndez JA. An overview of novel technologies to valorise coke oven gas surplus. Fuel Process Technol 2013;110:150–9.

[30] Ramírez-Santos ÁA, Castel C, Favre E. A review of gas separation technologies within emission reduction programs in the iron and steel sector: Current application and development perspectives. Sep Purif Technol 2018;194:425–42.

[31] Chen WH, Lin MR, Leu TS, Du SW. An evaluation of hydrogen production from the perspective of using blast furnace gas and coke oven gas as feedstocks. Int J Hydrogen Energy 2011;36:11727–37.

[32] Matteucci S, Yampolskii Y, Freeman BD, Pinnau I. Transport of gases and vapors in glassy and rubbery polymers. In: Yampolskii Y, Pinnau I, Freeman BD, editors. Materials Science of Membranes for Gas and Vapor Separation, Hoboken, NJ: John Wiley & Sons; 2006, p. 1–47.

[33] Yampolskii Y, Finkelshtein E. Permeability of polymers. In: Yampolskii Y, Finkelshtein E, editors. Membrane Materials for Gas and Vapor Separation., Hoboken, NJ:: John Wiley & Sons; 2017, p. 1–15.

[34] Perry JD, Nagai K, Koros WJ. Polymer membranes for hydrogen separations. MRS Bull 2006;31:745–9.

[35] Shao L, Low BT, Chung TS, Greenberg AR. Polymeric membranes for the

682 hydrogen economy: Contemporary approaches and prospects for the
683 future. J Memb Sci 2009;327:18–31.

684 [36] Basu S, Khan AL, Cano-Odena A, Liu C, Vankelecom IFJ. Membrane-
685 based technologies for biogas separations. Chem Soc Rev 2010;39:750–
686 68.

687 [37] Bounaceur R, Berger E, Pfister M, Ramirez Santos AA, Favre E. Rigorous
688 variable permeability modelling and process simulation for the design of
689 polymeric membrane gas separation units: MEMSIC simulation tool. J
690 Memb Sci 2017;523:77–91.

691 [38] Yong WF, Chung TS, Weber M, Maletzko C. New polyethersulfone (PESU)
692 hollow fiber membranes for CO2 capture. J Memb Sci 2018;552:305-14.

693 [39] Thornton A. Polymer gas separation membrane database. Membrane
694 Society of Australasia. https://membrane-australasia.org/msa-
695 activities/polymer-gas-separation-membrane-database/ [accessed in
696 November 2019]

697 [40] McCandless FP. Separation of binary mixtures of CO and H2 by
698 permeation through polymeric films. Ind Eng Chem Process Des Dev
699 1972;11:470–8.

700 [41] Hinchliffe AB. Separation of hydrogen carbon monoxide using polymer
701 membranes. PhD Thesis. Aston University, 1991.

702 [42] Peer M, Kamali SM, Mahdeyarfar M, Mohammadi T. Separation of
703 hydrogen from carbon monoxide using a hollow fiber polyimide membrane:
704 Experimental and simulation. Chem Eng Technol 2007;30:1418–25.

705 [43] David OC, Gorri D, Urtiaga A, Ortiz I. Mixed gas separation study for the
706 hydrogen recovery from H2/CO/N2/CO2 post combustion mixtures using a
707 Matrimid membrane. J Memb Sci 2011;378:359–68.

708 [44] Zarca G, Ortiz I, Urtiaga A. Copper(I)-containing supported ionic liquid
709 membranes for carbon monoxide/nitrogen separation. J Memb Sci
710 2013;438:38–45.

711 [45] Galizia M, Chi WS, Smith ZP, Merkel TC, Baker RW, Freeman BD. 50th
712 Anniversary Perspective: Polymers and mixed matrix membranes for gas
713 and vapor separation: A review and prospective opportunities.
714 Macromolecules 2017;50:7809–43.

715 [46] Robeson LM. Correlation of separation factor versus permeability for
716 polymeric membranes. J Memb Sci 1991;62:165–85.

717 [47] Robeson LM. The upper bound revisited. J Memb Sci 2008;320:390–400.

[48] Kumbharkar SC, Karadkar PB, Kharul UK. Enhancement of gas permeation properties of polybenzimidazoles by systematic structure architecture. J Memb Sci 2006;286:161–9.

[49] Abetz V, Brinkmann T, Dijkstra M, Ebert K, Fritsch D, Ohlrogge K, et al. Developments in membrane research: From material via process design to industrial application. Adv Eng Mater 2006;8:328–58.

[50] García MG, Marchese J, Ochoa NA. Improved gas selectivity of polyetherimide membrane by the incorporation of PIM polyimide phase. J Appl Polym Sci 2017;134:1–11.

[51] Koolivand H, Sharif A, Kashani MR, Karimi M, Salooki MK, Semsarzadeh MA. Functionalized graphene oxide/polyimide nanocomposites as highly CO2-selective membranes. J Polym Res 2014;21:1–12.

[52] Wang D. Polyethersulfone hollow fibre gas separation membranes prepared from solvent systems containing onsolvent additives. Doctoral Thesis. National University of Singapore, 1996.

[53] Li Y, Chung TS. Highly selective sulfonated polyethersulfone (SPES)-based membranes with transition metal counterions for hydrogen recovery and natural gas separation. J Memb Sci 2008;308:128–35.

[54] Products PP. Datasheet Polybenzimidazole. 2017.

[55] Hao L, Li P, Chung TS. PIM-1 as an organic filler to enhance the gas separation performance of Ultem polyetherimide. J Memb Sci 2014;453:614–23.

[56] Xia J, Liu S, Pallathadka PK, Chng ML, Chung TS. Structural determination of Extem XH 1015 and its gas permeability comparison with polysulfone and Ultem via molecular simulation. Ind Eng Chem Res 2010;49:12014–21.

[57] Wang Y, Jiang L, Matsuura T, Chung TS, Goh SH. Investigation of the fundamental differences between polyamide-imide (PAI) and polyetherimide (PEI) membranes for isopropanol dehydration via pervaporation. J Memb Sci 2008;318:217–26.

[58] Barbari TA, Koros WJ, Paul DR. Polymeric membranes based on bisphenol-A for gas separations. J Memb Sci 1989;42:69–86.

[59] Li Y, Chung T-S. Silver ionic modification in dual-layer hollow fiber membranes with significant enhancement in CO2/CH4 and O2/N2 separation. J Memb Sci 2010;350:226–31.

[60] Huang Z, Li Y, Wen R, Teoh MM, Kulprathipanja S. Enhanced gas

754 separation properties by using nanostructured PES-zeolite 4A mixed matrix
755 membranes. J Appl Polym Sci 2006;101:3800–5.

756 [61] Li X, Singh RP, Dudeck KW, Berchtold KA, Benicewicz BC. Influence of
757 polybenzimidazole main chain structure on H2/CO2 separation at elevated
758 temperatures. J Memb Sci 2014;461:59–68.

759 [62] Nadakatti SM, Kim JH, Stern SA. Solubility of light gases in poly(n-butyl
760 methacrylate) at elevated pressures. J Memb Sci 1995;108:279–91.

761 [63] Malagón-Romero DH, Ladino A, Ortiz N, Green LP. Characterization of a
762 polymeric membrane for the separation of hydrogen in a mixture with CO2.
763 Open Fuels Energy Sci J 2016;9:126–36.

764 [64] Shishatskiy S, Nistor C, Popa M, Nunes SP, Peinemann KV. Polyimide
765 asymmetric membranes for hydrogen separation: Influence of formation
766 conditions on gas transport properties. Adv Eng Mater 2006;8:390–7.

767 [65] Yong WF, Chung TS, Weber M, Maletzko C. New polyethersulfone (PESU)
768 hollow fiber membranes for CO2 capture. J Memb Sci 2018;552:305–14.

769 [66] El-Azzami LA, Grulke EA. Dual mode model for mixed gas permeation of
770 CO2, H2, and N2 through a dry chitosan membrane. J Polym Sci Part B
771 Polym Phys 2007;45:2620–31.

772 [67] Tanaka K, Kita H, Okamoto K, Nakamura A, Kusuki Y. Gas permeability
773 and permselectivity in polyimides based on 3,3',4,4'-
774 biphenyltetracarboxylic dianhydride. J Memb Sci 1989;47:203–15.

775 [68] Marchese J, Garis E, Anson M, Ochoa NA, Pagliero C. Gas sorption,
776 permeation and separation of ABS copolymer membrane. J Memb Sci
777 2003;221:185–97.

778 [69] Mohamad IN, Rohani R, Mastarmasdar MS, Mohd Nor MT, Md. Jahim J.
779 Permeation properties of polymeric membranes for biohydrogen
780 purification. Int J Hydrogen Energy 2016;41:4474–88.

781 [70] Hamid MAA, Chung YT, Rohani R, Junaidi MUM. Miscible-blend
782 polysulfone/polyimide membrane for hydrogen purification from palm oil
783 mill effluent fermentation. Sep Purif Technol 2019;209:598–607.

784 [71] David OC, Gorri D, Nijmeijer K, Ortiz I, Urtiaga A. Hydrogen separation from
785 multicomponent gas mixtures containing CO, N2 and CO2 using Matrimid
786 ® asymmetric hollow fiber membranes. J Memb Sci 2012;419–420:49–56.

787 [72] Sadrzadeh M, Amirilargani M, Shahidi K, Mohammadi T. Pure and mixed
788 gas permeation through a composite polydimethylsiloxane membrane.
789 Polym Adv Technol 2011;22:586–97.

790

791

792 **FIGURES**

814 **TABLES**

820